



# Chromosomal Mapping of Tandem Repeats Revealed Massive Chromosomal Rearrangements and Insights Into *Senna tora* Dysploidy

Nomar Espinosa Waminal<sup>1</sup>, Remnyl Joyce Pellerin<sup>1</sup>, Sang-Ho Kang<sup>2</sup> and Hyun Hee Kim<sup>1\*</sup>

<sup>1</sup> Department of Chemistry and Life Science, BioScience Institute, Sahmyook University, Seoul, South Korea, <sup>2</sup> Genomics Division, National Institute of Agricultural Sciences, Rural Development Administration, Jeonju, South Korea

## OPEN ACCESS

### Edited by:

Susann Wicke,  
Humboldt University of  
Berlin, Germany

### Reviewed by:

Eva Hribova,  
Academy of Sciences of the Czech  
Republic, Czechia  
Sònia García,  
Consejo Superior de Investigaciones  
Científicas (CSIC), Spain

### \*Correspondence:

Hyun Hee Kim  
kimhh@syu.ac.kr

### Specialty section:

This article was submitted to  
Plant Systematics and Evolution,  
a section of the journal  
Frontiers in Plant Science

**Received:** 16 November 2020

**Accepted:** 21 January 2021

**Published:** 10 February 2021

### Citation:

Waminal NE, Pellerin RJ, Kang S-H  
and Kim HH (2021) Chromosomal  
Mapping of Tandem Repeats  
Revealed Massive Chromosomal  
Rearrangements and Insights Into  
*Senna tora* Dysploidy.  
*Front. Plant Sci.* 12:629898.  
doi: 10.3389/fpls.2021.629898

Tandem repeats can occupy a large portion of plant genomes and can either cause or result from chromosomal rearrangements, which are important drivers of dysploidy-mediated karyotype evolution and speciation. To understand the contribution of tandem repeats in shaping the extant *Senna tora* dysploid karyotype, we analyzed the composition and abundance of tandem repeats in the *S. tora* genome and compared the chromosomal distribution of these repeats between *S. tora* and a closely related euploid, *Senna occidentalis*. Using a read clustering algorithm, we identified the major *S. tora* tandem repeats and visualized their chromosomal distribution by fluorescence *in situ* hybridization. We identified eight independent repeats covering ~85 Mb or ~12% of the *S. tora* genome. The unit lengths and copy numbers had ranges of 7–5,833 bp and 325–2.89 × 10<sup>6</sup>, respectively. Three short duplicated sequences were found in the 45S rDNA intergenic spacer, one of which was also detected at an extra-NOR locus. The canonical plant telomeric repeat (TTTAGGG)<sub>n</sub> was also detected as very intense signals in numerous pericentromeric and interstitial loci. StoTR05\_180, which showed subtelomeric distribution in *Senna occidentalis*, was predominantly pericentromeric in *S. tora*. The unusual chromosomal distribution of tandem repeats in *S. tora* not only enabled easy identification of individual chromosomes but also revealed the massive chromosomal rearrangements that have likely played important roles in shaping its dysploid karyotype.

**Keywords:** satellite DNA, *Senna tora*, tandem repeats, dysploidy, fluorescence *in situ* hybridization, whole genome duplication, karyotype

## INTRODUCTION

Numerous genome studies have shown the ubiquity and abundance of repetitive elements in plant genomes and have validated the crucial role of repeats in genome structure, function, and evolution (Wicker et al., 2007; Shatskikh et al., 2020). Once notoriously labeled as “junk DNA,” repetitive elements are now known as important players in gene regulation, stress response, and genome stability (Fedoroff, 2012). However, the same repeats are also substrates for, and byproducts of, chromosomal rearrangements, thereby driving variations in chromosome structure between closely related lineages (Schubert and Lysak, 2011; Murat et al., 2017). Tracing the dynamics of different repeat families among closely related taxa could therefore provide insights into a genome’s evolutionary past (Long et al., 2013; Waminal et al., 2018b).

Repetitive elements are classified into two major types: dispersed repeats and tandem repeats. Dispersed repeats, such as transposable elements, are scattered either sparsely or extensively in one or more genomic loci without following a head-to-tail organization (Frello and Heslop-Harrison, 2000). In contrast, tandem repeats follow a head-to-tail organization in one or more genomic loci. They include microsatellites (2–5 bp of usually 10–100 units), minisatellites (6–100 bp of 0.5–30 kb arrays), and longer satellites with varied unit lengths (usually 150–400 bp) and array size of up to several megabase pairs (Mehrotra and Goyal, 2014; Garrido-Ramos, 2017).

Tandem repeats are abundant in heterochromatic regions of chromosomes, such as the (peri)centromere and (sub)telomere. Although a single satellite family often dominates either of these chromosomal regions (Garrido-Ramos, 2017), many other repeats occupy these sites at low copies forming a library of repeats that could amplify at any favorable time, such as in response to genomic shock (Fedoroff and Bennetzen, 2013; Ruiz-Ruano et al., 2016). Moreover, ectopic (non-allelic) (micro)homologies between the (peri)centromere and (sub)telomere make these regions hotspots for chromosomal rearrangements (Salser et al., 1976; Kubis et al., 1998; Schubert and Lysak, 2011; Pellestor and Gatinois, 2018; Rosato et al., 2018; Hartley and O'Neill, 2019).

Chromosomal rearrangements may occur either intrachromosomally via segmental deletion, addition, or inversion, or interchromosomally via arm translocation, telomere-telomere “fusions” (also known as end-to-end translocation [EET]), and nested chromosome insertion (NCI) (Mandáková et al., 2019). Interchromosomal rearrangements can generate dysploid karyotypes, that is, altered chromosome numbers (Murat et al., 2010; Schubert and Lysak, 2011; Mandáková and Lysak, 2018). When chromosomes are fragmented and the fragments maintain or develop centromere function, species with increased chromosome numbers (ascending dysploid) are produced (Rousselet et al., 2000; Chung et al., 2011; Mandáková and Lysak, 2018; Schubert et al., 2020). Conversely, EET and NCI could generate species with fewer chromosomes (descending dysploid) (Rousselet et al., 2000; Mandáková and Lysak, 2018). For example, EETs have been implicated in the karyotype evolution of the ant *Myrmecia pilosula* (Imai and Taylor, 1989), human (Ijdo et al., 1991), and many crucifers (Mandáková et al., 2017), whereas NCI is more prevalent in grasses (Luo et al., 2009; Murat et al., 2010). Moreover, dysploidy, particularly descending dysploidy, is more prevalent in angiosperms than originally thought (Sousa and Renner, 2015; Levin, 2020).

Although tandem repeats have the potential to generate chromosome rearrangements, they could also be a product of such rearrangements, that is, tandem repeats and chromosomal rearrangements are closely associated (Sousa and Renner, 2015; Louzada et al., 2020). Tandem repeats can also undergo massive amplification through concerted evolutionary processes, including unequal crossing over, replication slippage, gene conversion, or rolling circle replication of circular DNA (Charlesworth et al., 1994; Cohen and Segal, 2009; Rosato et al., 2018). Sometimes, novel repeat families arise after re-establishing

genome stability from stressful events, such as a whole-genome duplication (WGD) (Fedoroff, 2012), which sometimes generates new taxonomic lineages (Murat et al., 2010; Waminal et al., 2016). Because the fixation of tandem repeats in terms of abundance and chromosome location may vary across different taxa in a clade (Perumal et al., 2017), quantifying and chromosomal mapping of tandem repeats can provide useful data to understand genome history and species relationships.

The genus *Senna* (Family Leguminosae, Subfamily Caesalpiniaceae) comprises many anthraquinone-producing medicinal plants (Jang et al., 2007; Puri, 2018; Kang et al., 2020b). Specifically, *Senna tora* L. (Roxb) (syn. *Cassia tora* L.) has been used traditionally as a dyeing agent, tea, or herbal medicine in several Asian countries, such as India, China, and Korea, and is now gaining global attention, prompting its genome sequencing initiative (Puri, 2018; Kang et al., 2020a).

The predominant diploid chromosome number in *Senna* is  $2n = 28$ . However, species with descending dysploid karyotypes of  $2n = 22–26$  have also been reported, including *S. tora* with  $2n = 26$  chromosomes (Pellerin et al., 2019). The taxonomic classification of *S. tora* and its related species is still ambiguous (Marazzi et al., 2006), and although the genome of *S. tora* has been released recently, no comprehensive comparative genomics with related *Senna* species has been performed to understand its genome evolution (Kang et al., 2020a). Nevertheless, analyzing the abundance of repeats using short next-generation sequencing reads and their chromosomal distribution through fluorescence *in situ* hybridization (FISH) could provide relevant insights into the karyotype evolution and genome history of *S. tora* (Ruiz-Ruano et al., 2016; Novák et al., 2017).

Here, we performed *in silico* mining for high-abundance tandem repeats in the *S. tora* genome using  $0.1\times$  whole-genome short reads. We then visualized the chromosomal distribution through FISH using repeat-specific pre-labeled oligo probes (PLOP) to understand the composition and role of tandem repeats in *S. tora* karyotype evolution. Unconventional chromosomal distribution of *S. tora* tandem repeats, especially when compared with its closely related species, *Senna occidentalis*, provided cytogenetic evidence of past extensive chromosomal rearrangements that may have shaped the extant *S. tora* genome.

## MATERIALS AND METHODS

### Plant Samples

*S. occidentalis* and *S. tora* seeds were kindly provided by the Department of Herbal Crop Research, NIHHS, RDA, Eumseong 369–873, South Korea. Seeds were germinated in potting soil and incubated in the greenhouse at 24–26°C. Root tips were treated with 2 mM 8-hydroxyquinoline for 4 h, fixed with aceto-ethanol (1:3 v/v), and stored in 70% ethanol at 4°C until use.

### Chromosome Spread Preparation

Sporophytic metaphase chromosome slide preparations were performed according to the technique of Waminal et al. (2012) with some modifications. Briefly, meristematic tips (~2 mm) were digested in a 50  $\mu$ l pectolytic enzyme solution (2% Cellulase

RS [Duchefa, Haarlem, The Netherlands, C8003.001] and 1% Pectolyase Y-23 [Duchefa, P8004.0001] in 100 mM citrate buffer) for 2 h at 37°C, and washed with distilled water. Roots were then transferred into a microtube containing chilled Carnoy's solution and vortexed for 30 s at room temperature. After disposing of the supernatant, the pellet was resuspended in (9:1 v/v) acetone-ethanol. The cellular suspension was then pipetted onto clean glass slides prewarmed in a humid chamber. After air-drying, slides were fixed for 5 min in 2% formaldehyde (Vrana et al., 2012), quickly dipped into distilled water, and dehydrated using ascending concentrations of ethanol (70, 90, and 100%).

## Repeat Mining and Quantification

Paired-end reads (100 bp), about  $2.9\times$  of the 686 Mb *S. tora* genome (Ohri et al., 1986), were obtained from the International Cooperation Team, International Technology Cooperation Center, RDA, Jeonju 54875, South Korea. Read quality trimming, read sampling, and repeat clustering were carried out using TAREAN (Novák et al., 2017). All consensus sequences were generated by TAREAN except for the Sto\_5S rDNA, StoIGS\_463, StoIGS\_293, and StoIGS\_188. The 5S rDNA contig was identified from dnaLCW analysis (Kim et al., 2015) using CLC Genomics Workbench (CLC Inc., Aarhus, Denmark) and annotated by BLAST against the 5S rDNA database (Szymanski et al., 2016). StoIGS\_463, StoIGS\_293, StoIGS\_188, and other repeats in the IGS of 45S rDNA were identified using Tandem Repeats Finder (Benson, 1999) and BLAST (Altschul et al., 1990). Tandem repeats identified with TAREAN were named following a similar nomenclature as Ruiz-Ruano et al. (2016). The four 45S rDNA contigs generated by TAREAN were assembled manually using the CLC Genomics Workbench. Sequences were submitted to Genbank and accession numbers are shown in corresponding tables.

We quantified the copy number and genome proportion of each repeat by mapping  $2.7\times$  trimmed short reads to the consensus sequences of the tandem repeats using CLC Genomics Workbench (CLC Inc.) and normalized the values to the 686-Mb 1C genome size of *S. tora*. For the 45S rDNA, we used only the 5,833 bp coding region without the IGS for quantification because of the different repeats in the IGS that could distort quantification. Short repeats were concatenated to form longer arrays for efficient read mapping.

## Probe Design

To visualize the chromosomal distribution of the repeats, we designed pre-labeled oligonucleotide probes (PLOPs). PLOPs for StoTR01\_86, StoTR03\_178, StoTR04\_55, StoTR05\_180, StoTR06\_159, and StoIGS\_463 were designed using the CLC Main Workbench and were synthesized by Bioneer (Daejeon, South Korea). PLOPs previously developed for the coding regions of the 5S rDNA and 45S rDNA, and the *Arabidopsis*-type telomeric repeat, which has the same sequence as StoTR02\_7\_tel, were used to localize these repeats (Waminal et al., 2018a). Details of the designed PLOPs are summarized in **Supplementary Table 1**.

## FISH and Karyotyping

A rapid FISH method was performed for PLOP-labeled probes (Waminal et al., 2018a). For PCR amplicon probes labeled via nick-translation, FISH was performed according to a modified procedure of Waminal et al. (2020). Homologous chromosomes were identified based on their FISH signals, morphological characteristics, and lengths considering previous karyotype data for *S. tora* (Pellerin et al., 2019). Karyograms were created using Adobe Photoshop CS6, whereas the idiogram and other diagrams were generated using Adobe Illustrator CS6.

## RESULTS

### Tandem Repeats With Various Lengths Comprise >12% of the *S. tora* Genome

A total of eight tandem repeats were identified using both TAREAN and dnaLCW (**Table 1**). Short read clustering of approximately  $0.1\times$  of the 686 Mb *S. tora* genome (Ohri et al., 1986), using TAREAN, generated seven satellite consensus sequences (**Figure 1**, **Table 1**). Of these, three were minisatellites: the canonical (*Arabidopsis*-type) plant telomeric minisatellite (TTTAGGG)<sub>n</sub>, which we named StoTR02\_7\_tel, StoTR01\_86, and StoTR04\_55. Three were satellites (StoTR03\_178, StoTR05\_180, and StoTR06\_159), and one is the 45S rDNA coding sequence (Sto\_45S\_CDS).

Three other clusters from the TAREAN output were grouped with the Sto\_45S\_CDS into a single 45S rDNA supercluster. Assembling these clusters generated a 10,235 bp 45S rDNA consensus with a 5,833 bp coding sequence (CDS) and a 4,402 bp intergenic spacer (IGS, **Figure 2A**, **Table 1**). The TAREAN pipeline was not able to generate any cluster associated with the 5S rDNA, indicating a low copy number in the *S. tora* genome. Therefore, to assemble the 5S rDNA sequence, we performed a *de novo* assembly of  $2.7\times$  short reads using the dnaLCW method (Kim et al., 2015). This approach enabled the identification of a 181 bp 5S rDNA contig, Sto\_5S (**Figure 2B**, **Table 1**).

All eight tandem repeats represented 0.01~3.93%, totaling 12.4%, of the *S. tora* genome (**Table 1**). In terms of total physical length, five repeats covered >7 Mb or >1% genome proportion (GP) (**Table 1**). StoTR01\_86 covered ~27 Mb or 3.9% GP followed by StoTR02\_7\_tel (~20 Mb, 2.7%), StoTR03\_178 (~15.2 Mb, 2.2%), StoTR04\_55 (~10.7 Mb, 1.6%), and Sto\_45S\_CDS (~7.1 Mb, 1.0%). Because of the various repeats in the 45S rDNA IGS which could potentially distort quantification (see below), we only used the CDS for 45S rDNA length and GP estimation. The actual values are expected to be higher. The other three repeats each had <1% GP, of which Sto\_5S had the lowest values for length and GP at 87.4 kb and 0.01%, respectively.

Shorter REs tended to have higher copy number. The shortest repeat, StoTR02\_7\_tel, showed the highest copies at  $2.89\times 10^6$  followed by StoTR01\_86 ( $3.13\times 10^5$ ), StoTR04\_55 ( $1.92\times 10^5$ ), StoTR03\_178 ( $8.56\times 10^4$ ), StoTR06\_159 ( $1.44\times 10^4$ ), and StoTR05\_180 ( $1.38\times 10^4$ ). However, the short 5S rDNA which was only 181 bp was much fewer than the 5,833 bp 45S rDNA (325 vs. 1,225 copies, respectively).

**TABLE 1** | Independent tandem repeats identified in the *S. tora* genome.

No	Name	Analysis tool	Length (bp)	AT (%)	Copy no.	Length (kb) <sup>a</sup>	GP (%) <sup>b</sup>	Accession no.
1	StoTR01_86	TAREAN	86	65	313,414	26,953.6	3.93	MW143025
2	StoTR02_7_tel	TAREAN	7	57	2,888,813	20,221.7	2.95	MW143031
3	StoTR03_178	TAREAN	178	49	85,581	15,233.4	2.22	MW143027
4	StoTR04_55	TAREAN	55	71	194,692	10,708.1	1.56	MW143024
5	StoTR05_180	TAREAN	180	58	13,772	2,478.9	0.36	MW143028
6	StoTR06_159	TAREAN	159	47	14,432	2,294.7	0.33	MW143026
7	Sto_45S_CDS	TAREAN	5,833	45	1,225	7,148.2	1.04	MW143033
8	Sto_5S	dnaLCW	181	48	325	87.4	0.01	MW143032

<sup>a</sup>Length (kb) = copy number × repeat length/1,000.

<sup>b</sup>Genome Proportion = length/*S. tora* genome size (686 Mb) × 100.

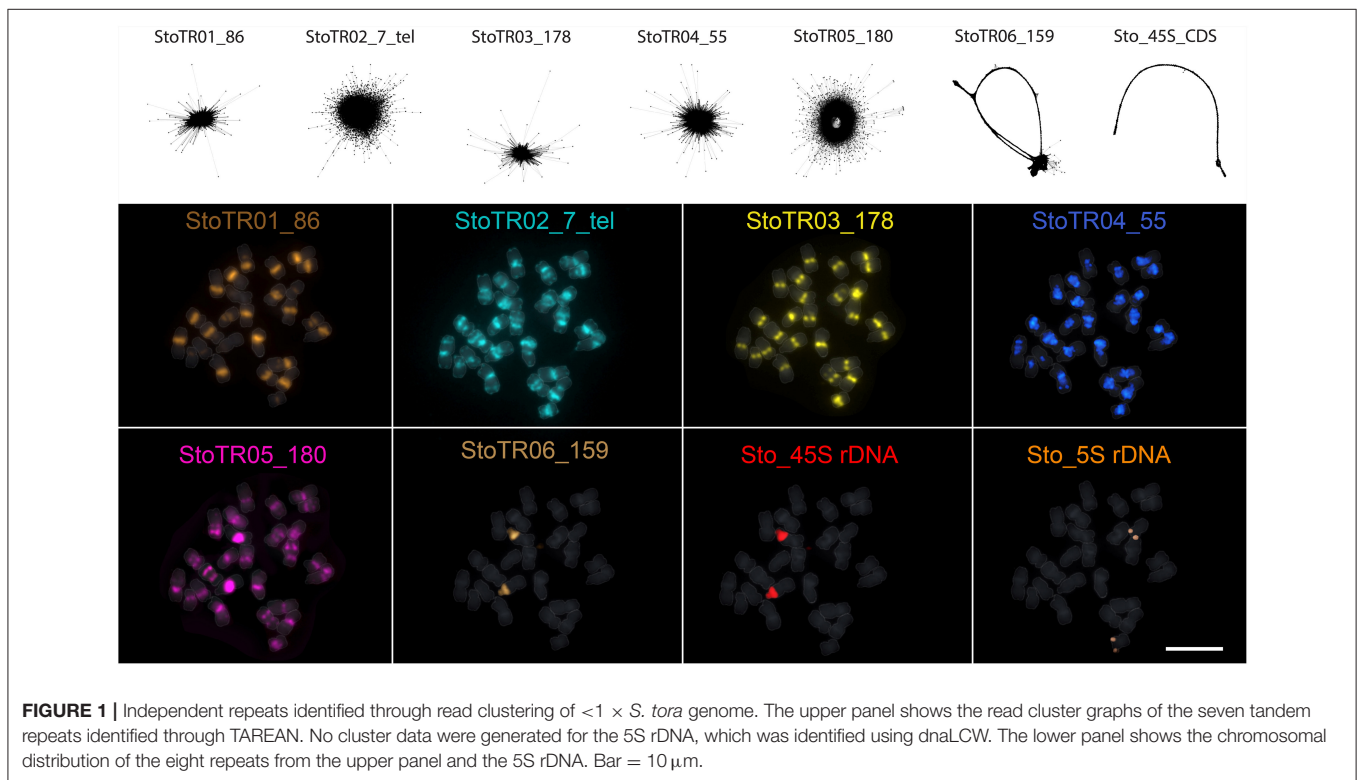


**FIGURE 1** | Independent repeats identified through read clustering of  $<1 \times S. tora$  genome. The upper panel shows the read cluster graphs of the seven tandem repeats identified through TAREAN. No cluster data were generated for the 5S rDNA, which was identified using dnaLCW. The lower panel shows the chromosomal distribution of the eight repeats from the upper panel and the 5S rDNA. Bar = 10  $\mu$ m.

## Short Duplicated Sequences Were Present in the Intergenic Spacer of *S. tora* 45S rDNA

We analyzed for the presence of duplicated sequences in the 4,402-bp 45S rDNA IGS region, considering that this region often carries different repeats and is known to be involved in genome reorganization in some species (Elliott et al., 2013; Havlová et al., 2016). We identified three  $>100$  bp short duplicated sequences (Figure 2A, Table 2). The longest was 463 bp long (StoIGS\_463) and was present in two copies but not tandemly arranged. The second was 293 bp long (StoIGS\_293) and was present in tandemly arranged 2.8 copies toward the 3' end of the IGS. The third was 188 bp long (StoIGS\_188) and was also tandemly arranged and distributed into two disjunct sites, each

immediately upstream of the StoIGS\_463. The upstream and downstream sites each had 2.0 and 0.6 copies of the StoIGS\_188. A short array of a 13 bp tandem repeat, StoIGS\_13, was also localized upstream of the 0.6-copy StoIGS\_188 locus.

Mapping of short reads to the 45S rDNA consensus sequence revealed a high coverage depth bias in the StoIGS\_188 regions (Figure 2A), which is indicative of either a collapsed IGS region in the consensus sequence or an extra-IGS homologous locus.

## StoTR06\_159 Is a Deletion Variant of StoIGS\_188

Our FISH results for StoTR06\_159 showed unexpected colocalization with the 45S rDNA locus (Figures 1, 3). Therefore, we mapped the StoTR06\_159 PLOPs to the Sto\_45S



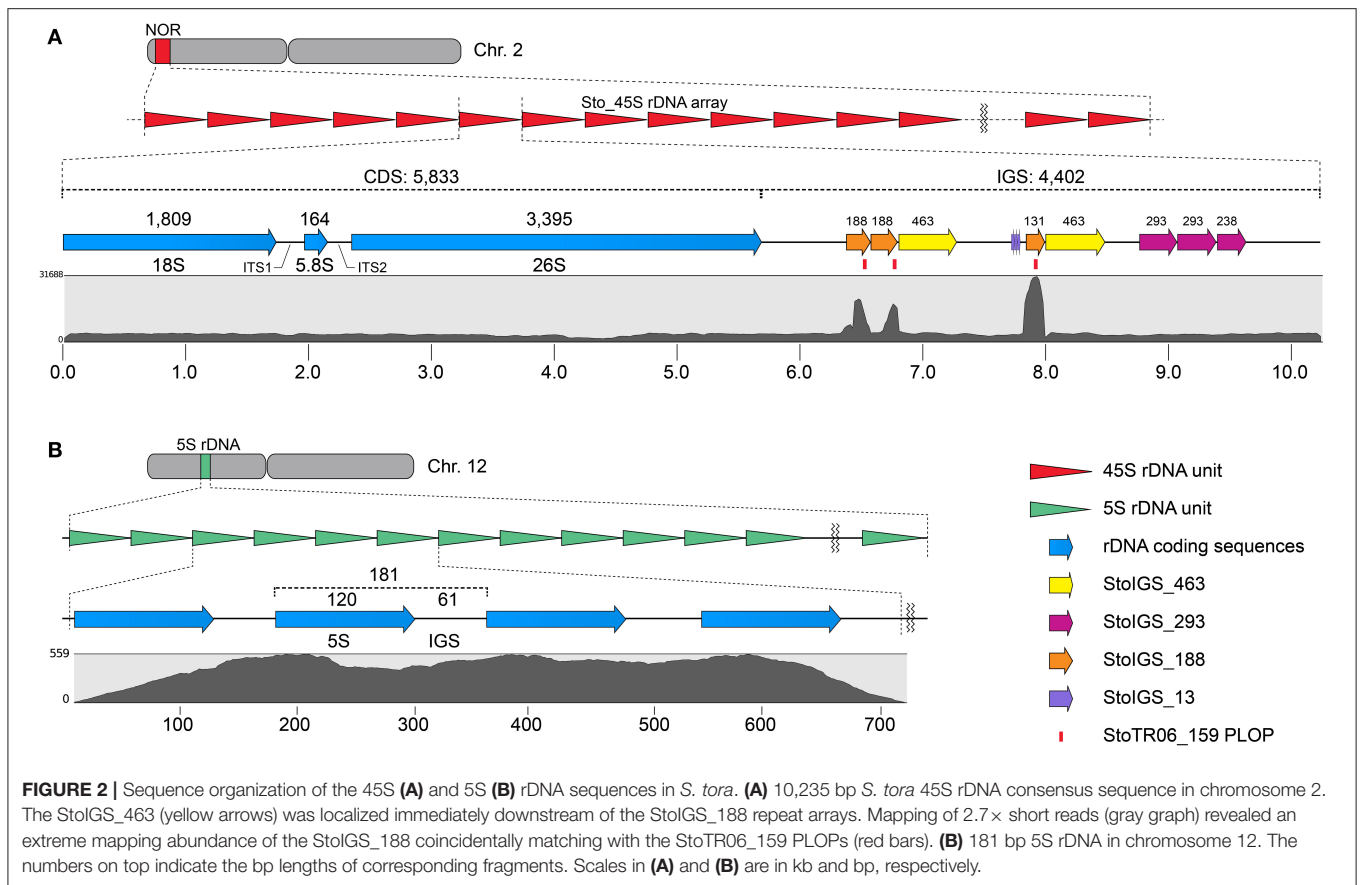


**TABLE 2 |** Short duplicated sequences identified in the 45S rDNA intergenic spacer using Tandem Repeats Finder.

No	Name	Type	Length (bp)	AT (%)	Copy no.	Length (kb) <sup>a</sup>	GP (%) <sup>b</sup>	Accession no.
1	StoIGS_463	IGS-related	463	65	2,612	1,209.2	0.18	MW143034
2	StoIGS_293	IGS-related	293	45	3,292	964.7	0.14	MW143035
3	StoIGS_188	IGS-related	188	48	3,856	724.9	0.11	MW143036

<sup>a</sup>Length (kb) = copy number  $\times$  repeat length/1,000.

<sup>b</sup>Genome Proportion = length/*S. tora* genome size (686 Mb)  $\times$  100.

consensus sequence to identify regions of homology between StoTR06\_159 and Sto\_45S. Interestingly, the PLOPs mapped to the deep-coverage StoIGS\_188 regions indicating sequence homology between StoIGS\_188 and StoTR06\_159 (**Figure 2A**). A sequence comparison between these two TRs revealed up to  $\sim 76\%$  identity mostly caused by deletions in StoTR06\_159 (**Supplementary Figure 1**). Three deletions were identified totaling 29 bp (9, 10, and 10 bp each) at 4–12, 41–50, and 82–91 nt. Outside these deletions, both TRs showed  $>87\%$  identity.

### FISH Revealed Predominant (peri)centromeric Distribution of *S. tora* Tandem Repeats

Five of the eight tandem repeats (StoTR01\_86, StoTR02\_7\_tel, StoTR03\_178, StoTR04\_55, StoTR05\_180), which accounted

for  $>11\%$  GP, showed predominantly (peri)centromeric distribution (**Figure 3A**, **Table 3**). StoTR01\_86, which had the highest genome proportions among all repeats, showed nine major and three minor loci. All major loci were exclusively paracentromeric at either the short (S) or long (L) arms of these nine chromosomes. The minor signal on Chr. 11 was pericentromeric, whereas those on chromosomes 4, 9, and 12 were paracentromeric (**Table 3**).

StoTR02\_7\_tel, an *Arabidopsis*-type telomeric repeat, was unusually abundant in the *S. tora* genome, in both repeat clustering quantification and FISH (**Figure 3**, **Table 1**). In addition to the canonical distribution at all chromosome termini, the StoTR02\_7\_tel FISH signals were intense in the pericentromeric region of all chromosomes. Although distinguishing the active centromere from the pericentromeric region was not straightforward in highly condensed metaphase

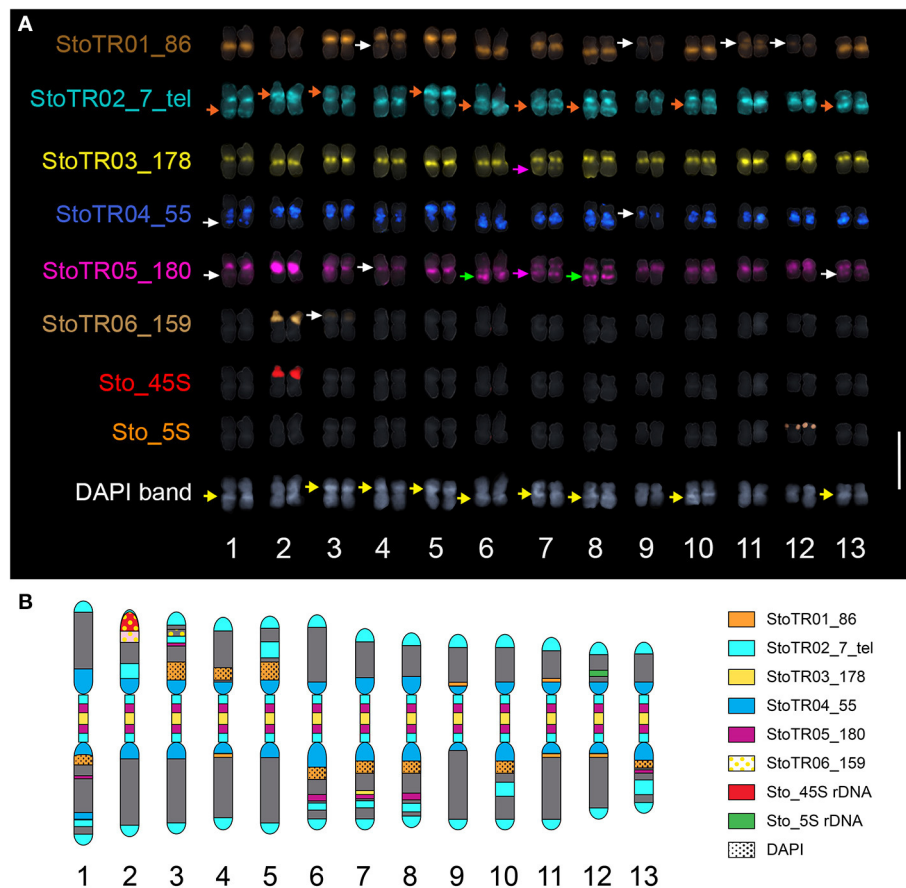


**FIGURE 3 |** Mitotic metaphase FISH karyogram of *S. tora*. **(A)** Chromosomal distribution of the eight independent tandem repeats showing mostly centromeric and pericentromeric localization. StoTR01\_86 localized at paracentric regions of either short or long arms, except for chromosomes 4 and 11 which showed pericentric localization. StoTR02\_7\_tel showed extra-telomeric signals at the centromere and interstitial regions of either, but not both, chromosome arms (orange arrows). StoTR03\_178 localized at centromeres of all chromosomes and at a weak locus in 7L which colocalized with StoTR05\_180 (pink arrows). StoTR04\_55 localized at pericentromeric regions in all chromosomes and a weak locus in 1L. StoTR05\_180 was intense in the centromere of chromosome 2. Aside from centromeric regions, it was also observed at equilocal sites in the interstitial regions of some chromosomes (green, white, and pink arrows). StoTR06\_159 showed an intense signal at the NOR site in chromosome 2S and a weak signal in chromosome 3S. One locus each was observed for the 45S and 5S rDNA families. Some chromosomes have inherent DAPI bands (yellow arrows). Note the colocalized StoTR06\_159 and the NOR site in chromosome 2S. White arrows indicate weak signals. Bar = 10  $\mu$ m. **(B)** Karyotype ideogram of *S. tora* with stretched (peri)centromeric region. Chromosomal niches of different repeats are indicated by different colors and patterns. The dark gray background indicates the DAPI counterstain.

chromosomes, we considered the StoTR02\_7\_tel loci as pericentromeric because active centromeres are unlikely to carry telomeric repeats, but instead have homogenous tandem repeats like those of StoTR03\_178 (Hartley and O'Neill, 2019). Moreover, upon closer examination, StoTR02\_7\_tel signals do not perfectly coincide with those of StoTR\_178 (Figure 3A). In addition to these pericentromeric loci, nine chromosomes carry roughly equilocal StoTR02\_7\_tel loci at either, but not both, short or long arms (2S, 3S, 5S, 1L, 6L, 7L, 8L, 10L, and 13L) (Table 3). Equilocality of repeats at interstitial regions in a chromosome are often relics of repeat displacement from the subtelomere (Garrido-Ramos, 2015).

StoTR03\_178 showed two distinct FISH signals at all metaphase chromosome centromeres, one per sister chromatid (Figure 3). The signal in chromosome 12 was noticeably more

intense than those in other centromeres, and a weak signal was observed in the interstitial region of chromosome 7L. Although we did not perform immunostaining for CENH3, the hallmark of an active centromere (Kursel and Malik, 2016), for lack of *S. tora*-specific CENH3 antibody, it is likely that StoTR03\_178 could be involved in active centromere function because of its abundant copies and distinct FISH signals characterizing functional regional centromeres (Schubert et al., 2020). StoTR05\_180 was detected in all chromosome pericentromeres and some interstitial regions. The centromeric signal in chromosome 2 was more intense than in other chromosomes. In addition to the centromeric loci, five equilocal interstitial loci were observed in five chromosomes: 1L, 6L, 7L, 8L, and 13L. Signals from 1L to 13L were weak and that of 7L was colocalized with StoTR03\_178 (Figure 3).

**TABLE 3** | Chromosomal distribution of the DNA repeats identified in the *S. tora* genome.

No	Name	Loci <sup>a</sup>	Chromosomal distribution
1	StoTR01_86	9/4	Major: paracentromeric on 9 chromosomes, 3 on short (S), and 6 on long (L) arms: (1L, 3S, 4S, 5S, 6L, 7L, 8L, 10L, and 13L). Minor: pericentromeric on chr. 11 and paracentromeric on 4L, 9S, and 12L
2	StoTR02_7_tel	13	Chromosome termini, pericentromeric in all chromosomes, interstitial on 1L, 2S, 3S, 5S, 6L, 7L, 8L, 10L, and 13L
3	StoTR03_178	13/1	Major: centromeric in all chromosomes, Chr. 12 more intense Minor: interstitial on 7L
4	StoTR04_55	12/2	Major: pericentromeric in all chromosomes except Chr. 9 Minor: pericentromeric in Chr. 9, interstitial on 1L
5	StoTR05_180	12/3	Major: centromere of Chr. 2 most intense, all centromeres except for chromosome 4, interstitial regions of 6L, 7L, and 8L Minor: centromere of chromosome 4, an interstitial region of 1L and 13L
6	StoTR06_159	1/1	Major: NOR site at 2S Minor: interstitial region of 3S
7	Sto_45S_CDS	1	2S
8	Sto_5S	1	12S
9	StoIGS_463	1	Colocalized at NOR site at 2S

<sup>a</sup>Number of chromosomes bearing major/minor FISH signals.

StoTR04\_55 localized to the pericentromeric region in all chromosomes. Except for chromosome 9, all chromosomes had intense signals. In addition, a minor signal was observed in the interstitial region of chromosome 1L. The dispersed distribution of StoTR04\_55 is characteristic of pericentromeric retrotransposons found in other plants (Lim et al., 2007). StoTR06\_159 was not localized at the centromere but revealed a colocalized signal at the NOR site of chromosome 2S and a weak signal at the interstitial region of chromosome 3S.

Both Sto\_45S and Sto\_5S rDNA had only one locus each at chromosomes 2S and 12S, respectively, as previously reported (Pellerin et al., 2019).

### FISH Revealed Specific Localization of StoIGS\_463 at the 45S rDNA Locus

Because some repeats that have been identified in the 45S rDNA IGS region in *S. tora* and other plants have also been detected in other chromosomal loci via FISH [see StoTR06\_159 and Lim et al. (2004)], we checked whether this is the same case for StoIGS\_463, although we observed no evidence of biased abundance from read mapping (Figure 2A). Unlike StoIGS\_188/StoTR06\_159, which showed overabundance in read mapping and a weak FISH signal at chromosome 3S, StoIGS\_463 did not show any extra-NOR signal, suggesting its specific localization in the 45S rDNA IGS (Supplementary Figure 2). Moreover, although we did not perform FISH with StoIGS\_293, it is likely that it is also specific to the IGS based on the absence of depth variation in the read mapping similar to that of StoIGS\_463 (Figure 2A).

### StoTR03\_178 Is a More Abundant Centromeric Sequence Variant of StoTR05\_180

Centromeric repeats are often categorized into families, which share >80% identity between members, and superfamilies with

<80% identity with other families (Lim et al., 2007; Ruiz-Ruano et al., 2016; Hartley and O'Neill, 2019). We compared the consensus sequences of StoTR03\_178 and StoTR05\_180 to see whether they are evolutionarily related. StoTR03\_178 and StoTR05\_180 shared ~71% sequence identity, suggesting that these are two separate families in the same *S. tora* centromeric superfamily (Supplementary Figure 3). Moreover, sequences homologous to CENP-B box (CENP-B box-like), which play important roles in centromere function (Okada et al., 2007), were detected in both StoTR03\_178 and StoTR05\_180 (Supplementary Figure 3). However, only StoTR03\_178 carries a 7 bp palindromic dyad symmetry region, which could indicate active centromeric DNA (Kasinathan and Henikoff, 2018).

Moreover, StoTR03\_178 was ~6-fold more abundant than StoTR05\_180 in *S. tora* (Table 1). Although both showed centromeric distribution, StoTR03\_178 was more exclusively localized in the centromeres, whereas StoTR05\_180 was abundant in pericentromeric and interstitial regions (Figure 3, Table 3). In addition, while the overall identity between the two families was <80%, one StoTR05\_180 FISH probe, StTR180\_OP2, was ~82% identical with StoTR03\_178 (Supplementary Figure 3). This probe could not distinguish between StoTR03\_178 and StoTR05\_180 targets, which could explain the seemingly abundant StoTR05\_180 FISH loci compared with the *in-silico* quantification data (Table 1). Nevertheless, non-centromeric signals from StoTR05\_180, particularly at the interstitial regions of 1L, 6L, 7L, 8L, and 13L, along with the intense centromeric signal on chromosome 2, indicate the presence of cytologically exclusive niches occupied by the StoTR05\_180 family.

### Comparative FISH With *S. occidentalis* Revealed Extensive Chromosomal Rearrangements in *S. tora*

In our previous work, we showed that *S. occidentalis* has interstitial telomeric repeats although not as extensive as

in *S. tora* (Pellerin et al., 2019). To better understand the chromosomal relationship between *S. occidentalis* and *S. tora*, we performed a comparative FISH between these two species using StoTR02\_7\_tel and centromeric (StoTR03\_178 and StoTR05\_180) distribution (**Figure 4A**).

Both *S. occidentalis* and *S. tora* showed StoTR02\_7\_tel signals at the canonical sites of chromosome termini. However, aside from being detected in only three chromosomes in *S. occidentalis*, interstitial StoTR02\_7\_tel sites were much weaker in *S. occidentalis* than in *S. tora*. Moreover, we did not observe any pericentromeric StoTR02\_7\_tel signals in *S. occidentalis*. Conversely, the interstitial and pericentromeric telomere repeat signals in *S. tora* were more ubiquitous and more pronounced suggesting that these interstitial telomere repeat loci in *S. tora* could stretch several megabases (**Figure 4A**).

Another striking difference between *S. occidentalis* and *S. tora* is the chromosomal distribution of StoTR05\_180. In *S. occidentalis*, StoTR05\_180 was cytologically colocalized with StoTR02\_7\_tel at chromosome termini and at interstitial sites. Moreover, some chromosomes have weaker StoTR05\_180 signals than StoTR02\_7\_tel, indicating fewer copies (**Figure 4A**). In *S. tora*, terminal StoTR05\_180 was not detected, but the interstitial and pericentromeric StoTR05\_180 signals were considerably more intense.

## DISCUSSION

We identified eight tandem repeats in the *S. tora* genome through clustering of homologous reads from 1× whole-genome short reads. These repeats covered >12% of the *S. tora* genome. The striking differences in the chromosomal distribution of these repeats between *S. occidentalis* and *S. tora* (i) provides cytological evidence of extensive chromosomal rearrangements that have occurred during *S. tora* speciation, (ii) highlights the roles of tandem repeats in these rearrangements, and (iii) offer a system for identifying individual *S. tora* chromosomes for karyotyping and cytotaxonomic studies.

### Roles of Tandem Repeats in *S. tora* Karyotype Evolution

The numerous ectopic and highly amplified tandem repeats in the (peri)centromeric and interstitial regions in *S. tora* chromosomes is evidence that they have been involved in shaping the extant *S. tora* genome (**Figure 4B**), either as a cause or, more likely, as a consequence of illegitimate recombination (Murat et al., 2010). This evidence, relative to that of *S. occidentalis* includes: (i) the ectopic loci of interstitial and pericentromeric telomeric repeats sites besides the canonical terminal telomeric sites, (ii) the displacement of StoTR05\_180 from subtelomeric in *S. occidentalis* to interstitial and pericentromeric sites in *S. tora*; (iii) the amplification of StoTR03\_178 specifically in *S. tora*; (iv) the presence of StoTR06\_159 homologous sequences in the 45S rDNA IGS; and (v) the descending dysploid karyotype of *S. tora*.

First, interstitial telomeric repeats (ITR) have been observed in several plants, although some are not as extensive as what is seen

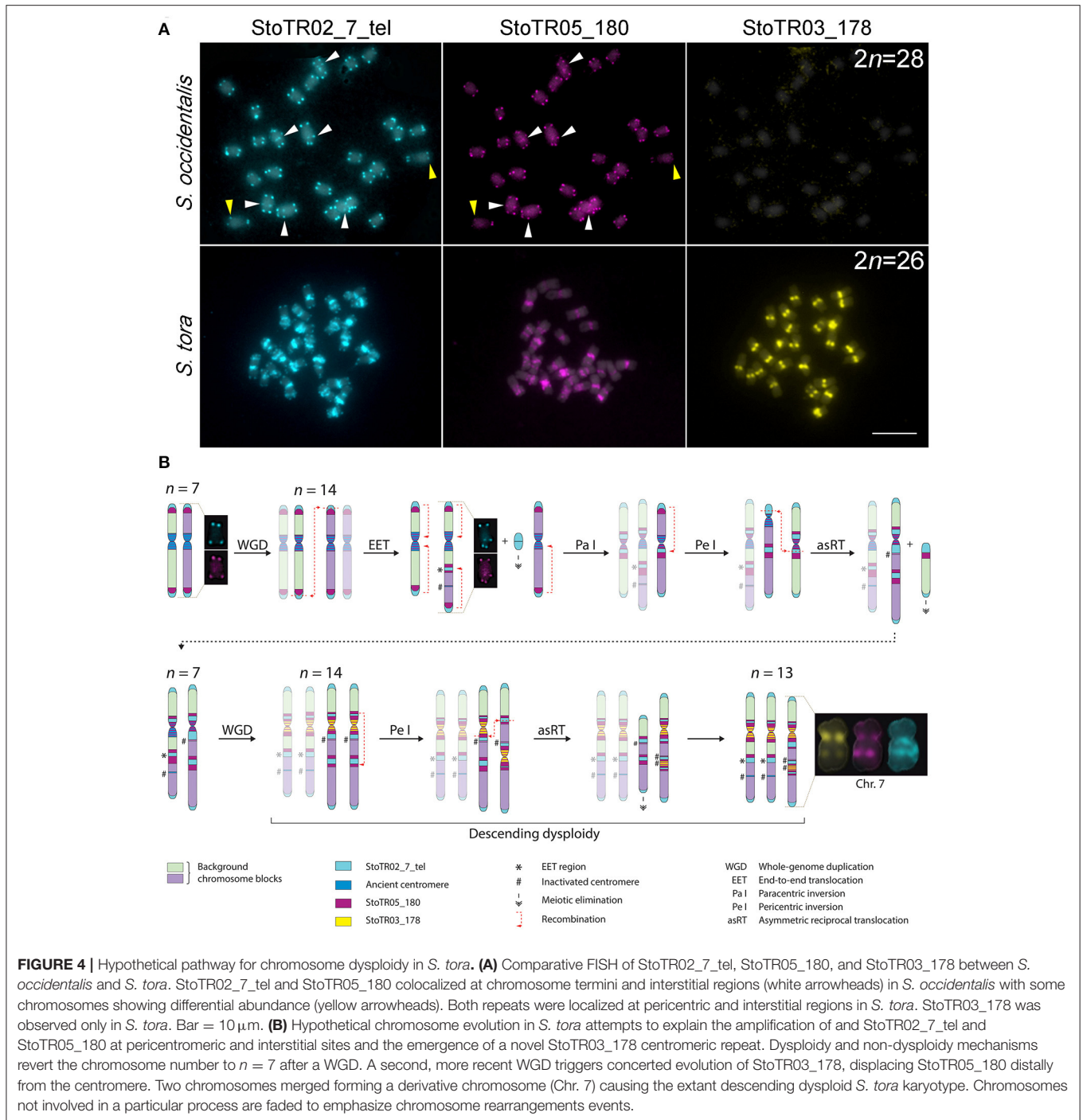
here in *S. tora* (Fuchs et al., 1995; He et al., 2013). These ITRs may have been generated via descending dysploid mechanisms such as end fusions (EET) and chromosome insertions (NCI), via chromosome inversions, or via amplification and reintegration of telomeric extrachromosomal circular DNA (eccDNA) repeats (Zellinger et al., 2007; Cohen and Segal, 2009). Although the replication, amplification, anchoring, and reintegration of eccDNAs into chromosomes have been demonstrated (Zellinger et al., 2007; Cohen and Segal, 2009; Durkin et al., 2012; Koo et al., 2018), we are careful not to speculate about their supposed contribution to generating interstitial and pericentromeric telomeric repeats in *S. tora* because there is limited information about the mechanisms of eccDNA-induced chromosome rearrangements in plants. Nevertheless, mechanisms involving eccDNA (Cohen and Segal, 2009) could help explain the amplification of ectopic telomeric repeats after they have moved to their new sites.

Alternatively, both EET and NCI could generate ITRs. However, EET is more plausible for explaining the situation in *S. tora* because all interstitial telomeric signals were observed only in one arm of all chromosomes bearing this signal, contrary to both arms if they were caused by NCI. However, we cannot rule out the possibility of NCI-mediated chromosome rearrangements, which, in this case, should require a biased reduction or elimination of the interstitial telomeric repeat array size in one arm, leaving signals in one arm undetectable by FISH (Majerová et al., 2014). Nevertheless, we believe that this is unlikely to happen compared with EET, considering the low likelihood for all chromosomes with interstitial telomeric loci to receive the same single-arm signals in a presumably random process of chromosomal rearrangements.

Second, whereas EET could generate interstitial telomeric and StoTR05\_180 loci, it does not explain the disappearance of subtelomeric StoTR05\_180 and its subsequent accumulation at pericentromeres as well as the concomitant accumulation of pericentromeric telomeric repeat loci in *S. tora*. Sequence microhomology between telomeres and centromeres (He et al., 2013; Pellestor and Gatinois, 2018) may have caused paracentric inversion with breakpoints at a proximal pericentromeric region and at terminal telomeric repeat loci (rather than at subtelomeric StoTR05\_180 loci), which then likely generated pericentromeric StoTR05\_180 at recombination sites followed by repeat array amplification. The subsequent disruption of (peri)centromere chromatin could have altered the epigenetic makeup of these regions, promoting centromere repositioning at pericentromeric StoTR05\_180 sites, as satellites are known targets for epigenetic *de novo* centromere formation (Okada et al., 2007; Schubert, 2018; Lu and He, 2019), and centromere repositioning is shown to be more frequent than originally thought (Mandáková et al., 2020). Repositioned kinetochore assembly at pericentromeric StoTR05\_180 sites likely seeded DNA mutation and amplification of StoTR03\_178 as a new centromeric repeat variant unique to *S. tora*.

Third, the fact that there are more abundant copies of StoTR03\_178 than there are of StoTR05\_180, in addition to its centromeric location, suggest a novel shift of centromeric repeat preference to StoTR03\_178 resulting from reestablishing





proper meiotic pairing after genomic shock (Ma and Gustafson, 2005; Schubert and Vu, 2016). Mutations in StoTR05\_180 sequences likely reduced its affinity to the kinetochore, thus weakening the centromere drive (Schubert, 2018). These mutations could have seeded StoTR03\_178, which may have developed a higher affinity for the *S. tora* kinetochore and eventually dominated the centromere, pushing the StoTR05\_180 to the pericentromeric regions, similar to

what has been observed in other plants (Hirsch and Jiang, 2012). In addition, StoTR03\_178 was completely absent in *S. occidentalis*, indicating a more recent amplification in the *S. tora* genome. Immunostaining with *S. tora* CENH3 should provide insights into the active centromere sites in *S. tora* chromosomes.

Fourth, 45S rDNA IGS is often linked to genome rearrangements (Havlová et al., 2016). Several duplicated

sequences in the 45S rDNA IGS region have been identified as independent satellites somewhere else in the genome, outside the 45S rDNA array, in several plants similar to the relationship between StoTR06\_159 and StoIGS\_188 (Almeida et al., 2012; Elliott et al., 2013; Kirov et al., 2018). This observation suggests the role of the 45S rDNA IGS as a “repeat carrier” during genome rearrangement. However, although some authors hypothesized that these repeats are from the IGS region, which then moved out and amplified in other chromosomal loci (Almeida et al., 2012), others hypothesize otherwise (Falquet et al., 1997). To date, there is no definitive conclusion to the directionality of IGS-related satellite evolution nor is there a conclusive mechanism to explain the process by which 45S rDNA IGS operates in this process (Almeida et al., 2012).

Lastly, the  $2n = 28$  chromosome number is predominant in *Senna* and lower numbers such as  $2n = 22–26$  are considered descending dysploid species (Cordeiro and Felix, 2017; Pellerin et al., 2019). In *S. tora*, this reduction is likely caused by a merger of two chromosomes, resulting in derivative chromosome 7, as indicated by the interstitial signal of StoTR03\_178 in chromosome 7L (Figure 3). The reduced chromosome number in *S. tora* indicates extensive genome rearrangements in *S. tora* relative to that of *S. occidentalis* (Figure 4B).

Chromosome rearrangements in many species often involve just one or a few chromosomes, contrary to all chromosomes rearranging all at once in a concerted manner (Mandáková and Lysak, 2018). However, chromoanagenic pathways, such as chromothripsis and chromoplexy, have been shown to produce massive chromosome rearrangements involving several chromosomes via dysploid and non-dysploid mechanisms in just a few generations (Comai and Tan, 2019; Pellestor and Gatinois, 2020). It is therefore interesting to know whether the extensive chromosomal rearrangements in *S. tora* occurred in a rapid process, or over slow recurrent rounds of hybridization. In addition, considering that *S. occidentalis* has three chromosomes with interstitial StoTR02\_7\_tel and StoTR05\_180, reconstructing the ancestral *Senna* karyotype will be necessary to understand karyotype evolution in *Senna*. Comprehensive comparative cytogenomic analyses in *Senna* are crucial to achieving this.

## A Hypothetical Chromosomal Evolution in *S. tora*

WGD is pervasive in angiosperms (Jiao et al., 2011; Soltis and Soltis, 2016). During the diploidization process, which a cell's mechanism for reestablishing proper meiotic pairing after a genomic shock from WGD (Ma and Gustafson, 2005; Schubert and Vu, 2016), karyotype dysploidy may occur (Levin, 2020). Recurrent cycles of WGD and diploidization in some lineages increased the chances of genome rearrangements and dysploidy, producing taxa with different chromosome numbers (Lysak et al., 2006; Mandáková et al., 2010; Mandáková et al., 2019; Symonds et al., 2010; Jiao et al., 2011; Chalhoub et al., 2014; Murat et al., 2017; Mandáková and Lysak, 2018).

In *Senna*,  $x = 7$  is considered as the base chromosome number after the discovery of *Senna rugosa* cytotypes with a haploid chromosome number of  $n = 7$  (Resende et al.,

2014), suggesting that species with the predominant  $2n = 28$  could technically be diploidized tetraploids. Comparing the chromosomal distribution of *S. tora* tandem repeats between *S. occidentalis* and *S. tora*, we hypothesize that the extant *S. tora* genome, like many angiosperms, has experienced at least two rounds of WGD in the immediate past. The diploidization that followed each WGD event may have differently influenced the *S. tora* karyotype temporally; such that, the former WGD may have radically reverted the chromosome number to the diploid count whereas the latter “fused” two chromosomes, generating the extant  $2n = 26$  dysploid karyotype (Figure 4B).

After an older WGD event, the chromosome number may have doubled to  $2n = 28$  from an ancestral  $2n = 14$  karyotype. Dysploidy and non-dysploidy mechanisms may have reverted the chromosome number to  $2n = 14$ ; a similar reversion of chromosomal number to diploid count has been observed between *Zea mays* and *Sorghum bicolor* (Murat et al., 2010; Freeling et al., 2012). A more recent WGD event may have doubled the chromosome number to  $2n = 28$ , which is then followed by EET of two chromosomes generating chromosome 7; hence, the extant  $2n = 26$  karyotype of *S. tora*.

Nevertheless, with purely molecular cytogenetic data, it is difficult to draw a definitive conclusion on the chromosome evolution of *S. tora*. The current genome assembly of *S. tora* and comparative genome analyses in *Senna* should provide more insight into *S. tora* chromosome evolution.

## Tandem Repeats for *Senna* Karyotyping and Cytogenetics

The chromosomal distribution of the major *S. tora* tandem repeats facilitated the identification of individual homologous chromosomes for karyotyping (Figure 3B, Supplementary Table 2). Because chromosomal rearrangements are less likely homoplastic, they can be used to infer phylogenetic relationships between species (Mandáková and Lysak, 2008). Repeats are used as species identifiers in cytotoxic studies (Guerra, 2008, 2012) because certain repeat families are widely distributed within a taxonomic family or genus, or even specific to a species, a genome, a tissue, or even a chromosome (Sharma and Raina, 2005; Ruban et al., 2014).

To gain a comprehensive understanding of the satellite repeat dynamics in *Senna*, a comprehensive comparative satellitome (Ruiz-Ruano et al., 2016) between *Senna* species will unravel clade- or species-specific abundant satellites in *Senna* not only for karyotyping but also for unraveling satellite dynamics and genome history in *Senna*.

## CONCLUSION

The identification and chromosomal mapping of the major tandem repeats in *S. tora* provided cytological evidence of past genome rearrangements. We have presented here the major tandem repeats that comprise and play an active role in shaping the highly rearranged descending dysploid *S. tora* karyotype. Using *in silico* and FISH data, we hypothesized an evolutionary pathway to the extant *S. tora* genome involving

dysploid and non-dysploid mechanisms. This chromosomal information should be complemented with molecular data because sequences used here were purely generated *in silico*. Amplification and sequencing of the >4 kb *S. tora* 45S rDNA IGS region should provide a more accurate description of the IGS structure, for example, discovery of phylogenetically important sequence variants that would help decipher not only subgenome relationships within *S. tora* but also with other *Senna* species. Moreover, comparison with different *Senna* species should provide further insights into the role of 45S rDNA in genome rearrangements. Lastly, phylogenomic analysis will allow testing for a correlation between chromosomal rearrangements and species divergence and trace major chromosomal events that have occurred during speciation in *Senna*.

To understand whether the repeats identified here are specific to *S. tora* or are conserved within the genus or its sub-lineages, comparative cytogenetic analyses with other related species are necessary. Moreover, whereas most repeats identified here are satellite DNAs, a comprehensive repeatomics (Macas et al., 2015) involving repeats like transposable elements in *S. tora* and other *Senna* species will be the focus of a future work to fully understand the repeat dynamics in *Senna*. The release of the *S. tora* genome should enable identification of the two donor chromosomes that contribute to the *S. tora* chromosome 7 and pave the way for reconstructing the ancestral *Senna* karyotype.

## REFERENCES

- Almeida, C., Fonseca, A., Dos Santos, K. G., Mosiolek, M., and Pedrosa-Harand, A. (2012). Contrasting evolution of a satellite DNA and its ancestral IGS rDNA in Phaseolus (Fabaceae). *Genome* 55, 683–689. doi: 10.1139/g2012-059
- Altschul, S. F., Gish, W., Miller, W., Myers, E. W., and Lipman, D. J. (1990). Basic local alignment search tool. *J. Mol. Biol.* 215, 403–410. doi: 10.1016/S0022-2836(05)80360-2
- Benson, G. (1999). Tandem repeats finder: a program to analyze DNA sequences. *Nucleic Acids Res.* 27, 573–580. doi: 10.1093/nar/27.2.573
- Chalhoub, B., Denoeud, F., Liu, S., Parkin, I. A. P., Tang, H., Wang, X., et al. (2014). Early allopolyploid evolution in the post-Neolithic Brassica napus oilseed genome. *Science* 345, 950–953. doi: 10.1126/science.1253435
- Charlesworth, B., Sniegowski, P., and Stephan, W. (1994). The evolutionary dynamics of repetitive DNA in eukaryotes. *Nature* 371, 215–220. doi: 10.1038/371215a0
- Chung, K. S., Weber, J. A., and Hipp, A. L. (2011). Dynamics of chromosome number and genome size variation in a cytogenetically variable sedge (*Carex scoparia* var. *scoparia*, Cyperaceae). *Am. J. Bot.* 98, 122–129. doi: 10.3732/ajb.1000046
- Cohen, S., and Segal, D. (2009). Extrachromosomal circular DNA in eukaryotes: possible involvement in the plasticity of tandem repeats. *Cytogenet. Genome Res.* 124, 327–338. doi: 10.1159/000218136
- Comai, L., and Tan, E. H. (2019). Haploid induction and genome instability. *Trends Genet.* 35, 791–803. doi: 10.1016/j.tig.2019.07.005
- Cordeiro, J. M. P., and Felix, L. P. (2017). Intra- and interspecific karyotypic variations of the genus *Senna* Mill (Fabaceae, Caesalpinoideae). *Acta Botanica Brasilica* 32, 128–134. doi: 10.1590/0102-33062017abb0274
- Durkin, K., Coppieters, W., Drögemüller, C., Ahariz, N., Cambisano, N., Druet, T., et al. (2012). Serial translocation by means of circular intermediates underlies colour sidedness in cattle. *Nature* 482, 81–84. doi: 10.1038/nature10757
- Elliott, T. A., Stage, D. E., Crease, T. J., and Eickbush, T. H. (2013). In and out of the rRNA genes: characterization of Pokey elements in the sequenced *Daphnia* genome. *Mob. DNA* 4:20. doi: 10.1186/1759-8753-4-20

## DATA AVAILABILITY STATEMENT

The datasets presented in this study can be found in online repositories. The names of the repository/repositories and accession number(s) can be found in the article/**Supplementary Material**.

## AUTHOR CONTRIBUTIONS

NW and HK conceived and designed the experiment. NW performed bioinformatics analyses. RP performed the FISH experiment. NW and RP wrote the manuscript. S-HK provided the whole genome sequence and plant samples. All authors approved the final manuscript.

## FUNDING

This study was funded by a grant from the National Research Foundation of Korea (NRF 2017R1A2B2004778).

## SUPPLEMENTARY MATERIAL

The Supplementary Material for this article can be found online at: <https://www.frontiersin.org/articles/10.3389/fpls.2021.629898/full#supplementary-material>

- Falquet, J., Creusot, F., and Dron, M. (1997). Molecular analysis of *Phaseolus vulgaris* rDNA unit and characterization of a satellite DNA homologous to IGS subrepeats. *Plant Physiol. Bioch.* 35, 611–622.
- Fedoroff, N. V. (2012). Presidential address. Transposable elements, epigenetics, and genome evolution. *Science* 338, 758–767. doi: 10.1126/science.338.6108.758
- Fedoroff, N. V., and Bennetzen, J. L. (2013). “Transposons, genomic shock, and genome evolution,” in *Plant Transposons and Genome Dynamics in Evolution*, ed N. V. Fedoroff (Hoboken, NJ: Wiley-Blackwell), 181–201. doi: 10.1002/9781118500156.ch10
- Freeling, M., Woodhouse, M. R., Subramaniam, S., Turco, G., Lisch, D., and Schnable, J. C. (2012). Fractionation mutagenesis and similar consequences of mechanisms removing dispensable or less-expressed DNA in plants. *Curr. Opin. Plant Biol.* 15, 131–139. doi: 10.1016/j.pbi.2012.01.015
- Frello, S., and Heslop-Harrison, J. S. (2000). Repetitive DNA sequences in *Crocus vernus* Hill (Iridaceae): The genomic organization and distribution of dispersed elements in the genus *Crocus* and its allies. *Genome* 43, 902–909. doi: 10.1139/g00-044
- Fuchs, J., Brandes, A., and Schubert, I. (1995). Telomere sequence localization and karyotype evolution in higher plants. *Plant Syst. Evol.* 196, 227–241. doi: 10.1007/BF00982962
- Garrido-Ramos, M. (2017). Satellite DNA: an evolving topic. *Genes* 8:230. doi: 10.3390/genes8090230
- Garrido-Ramos, M. A. (2015). Satellite DNA in plants: more than just rubbish. *Cytogenet. Genome Res.* 146, 153–170. doi: 10.1159/000437008
- Guerra, M. (2008). Chromosome numbers in plant cytotaxonomy: concepts and implications. *Cytogenet. Genome Res.* 120, 339–350. doi: 10.1159/000121083
- Guerra, M. (2012). Cytotaxonomy: the end of childhood. *Plant Biosyst.* 146, 703–710. doi: 10.1080/11263504.2012.717973
- Hartley, G., and O'Neill, R. (2019). Centromere repeats: hidden gems of the genome. *Genes* 10:223. doi: 10.3390/genes10030223
- Havlová, K., Dvoráčková, M., Peiro, R., Abia, D., Mozgová, I., Vansáčová, L., et al. (2016). Variation of 45S rDNA intergenic spacers in *Arabidopsis thaliana*. *Plant Mol. Biol.* 92, 457–471. doi: 10.1007/s11103-016-0524-1



- He, L., Liu, J., Torres, G. A., Zhang, H., Jiang, J., and Xie, C. (2013). Interstitial telomeric repeats are enriched in the centromeres of chromosomes in Solanum species. *Chromosome Res.* 21, 5–13. doi: 10.1007/s10577-012-9332-x
- Hirsch, C. D., and Jiang, J. (2012). "Centromeres: sequences, structure, and biology plant genome diversity" in *Plant Genome Diversity*, eds J. F. Wendel, J. Greilhuber, J. Dolezel, and I. J. Leitch (Vienna: Springer), 59–70.
- Ijdo, J. W., Baldini, A., Ward, D. C., Reeders, S. T., and Wells, R. A. (1991). Origin of human chromosome 2: an ancestral telomere-telomere fusion. *PNAS* 88, 9051–9055. doi: 10.1073/pnas.88.20.9051
- Imai, H. T., and Taylor, R. W. (1989). Chromosomal polymorphisms involving telomere fusion, centromeric inactivation and centromere shift in the ant Myrmecia (pilosula) n=1. *Chromosoma* 98, 456–460. doi: 10.1007/BF00292792
- Jang, D. S., Lee, G. Y., Kim, Y. S., Lee, Y. M., Kim, C.-S., Yoo, J. L., et al. (2007). Anthraquinones from the seeds of *Cassia tora* with inhibitory activity on protein glycation and aldose reductase. *Biol. Pharm. Bull.* 30, 2207–2210. doi: 10.1248/bpb.30.2207
- Jiao, Y., Wickett, N. J., Ayyampalayam, S., Chandrabali, A. S., Landherr, L., Ralph, P. E., et al. (2011). Ancestral polyploidy in seed plants and angiosperms. *Nature* 473, 97–100. doi: 10.1038/nature09916
- Kang, S.-H., Pandey, R. P., Lee, C.-M., Sim, J.-S., Jeong, J.-T., Choi, B.-S., et al. (2020a). Genome-enabled discovery of anthraquinone biosynthesis in *Senna tora*. *Nat. Commun.* 2020:063495. doi: 10.1101/2020.04.27.063495
- Kang, S. H., Lee, W. H., Lee, C. M., Sim, J. S., Won, S. Y., Han, S. R., et al. (2020b). *De novo* transcriptome sequence of *Senna tora* provides insights into anthraquinone biosynthesis. *PLoS ONE* 15:e0225564. doi: 10.1371/journal.pone.0225564
- Kasinathan, S., and Henikoff, S. (2018). Non-B-form DNA is enriched at centromeres. *Mol. Biol. Evol.* 35, 949–962. doi: 10.1093/molbev/msy010
- Kim, K., Lee, S.-C., Lee, J., Yu, Y., Yang, K., Choi, B.-S., et al. (2015). Complete chloroplast and ribosomal sequences for 30 accessions elucidate evolution of *Oryza* AA genome species. *Sci. Rep.* 5:15655. doi: 10.1038/srep15655
- Kirov, I., Gilyok, M., Knyazev, A., and Fesenko, I. (2018). Pilot satellitome analysis of the model plant, *Physcomitrella patens*, revealed a transcribed and high-copy IGS related tandem repeat. *Comp. Cytogenet.* 12, 493–513. doi: 10.3897/CompCytogen.v12i4.31015
- Koo, D.-H., Molin, W. T., Sasaki, C. A., Jiang, J., Putta, K., Jugulam, M., et al. (2018). Extrachromosomal circular DNA-based amplification and transmission of herbicide resistance in crop weed *Amaranthus palmeri*. *PNAS* 115, 3332–3337. doi: 10.1073/pnas.1719354115
- Kubis, S., Schmidt, T., and Heslop-Harrison, J. S. (1998). Repetitive DNA elements as a major component of plant genomes. *Ann. Bot.* 82, 45–55. doi: 10.1006/anbo.1998.0779
- Kursel, L. E., and Malik, H. S. (2016). Centromeres. *Curr. Biol.* 26, R487–R490. doi: 10.1016/j.cub.2016.05.031
- Levin, D. A. (2020). Did dysploid waves follow the pulses of whole genome duplications? *Plant Syst. Evol.* 306:75. doi: 10.1007/s00606-020-01704-5
- Lim, K. B., Yang, T. J., Hwang, Y. J., Kim, J. S., Park, J. Y., Kwon, S. J., et al. (2007). Characterization of the centromere and peri-centromere retrotransposons in *Brassica rapa* and their distribution in related Brassica species. *Plant J.* 49, 173–183. doi: 10.1111/j.1365-3113.2006.02952.x
- Lim, K. Y., Skalicka, K., Koukalova, B., Volkov, R. A., Matyasek, R., Hemleben, V., et al. (2004). Dynamic changes in the distribution of a satellite homologous to intergenic 26-18S rDNA spacer in the evolution of Nicotiana. *Genetics* 166, 1935–1946. doi: 10.1534/genetics.166.4.1935
- Long, Q., Rabanal, F. A., Meng, D., Huber, C. D., Farlow, A., Platzer, A., et al. (2013). Massive genomic variation and strong selection in *Arabidopsis thaliana* lines from Sweden. *Nature Genet.* 45, 884–890. doi: 10.1038/ng.2678
- Louzada, S., Lopes, M., Ferreira, D., Adegas, F., Escudeiro, A., Gama-Carvalho, M., et al. (2020). Decoding the role of satellite DNA in genome architecture and plasticity—an evolutionary and clinical affair. *Genes* 11:72. doi: 10.3390/genes11010072
- Lu, M., and He, X. (2019). Centromere repositioning causes inversion of meiosis and generates a reproductive barrier. *Proc. Natl. Acad. Sci. U. S. A.* 116, 21580–21591. doi: 10.1073/pnas.1911745116
- Luo, M. C., Deal, K. R., Akhunova, E. D., Akhunova, A. R., Anderson, O. D., Anderson, J. A., et al. (2009). Genome comparisons reveal a dominant mechanism of chromosome number reduction in grasses and accelerated genome evolution in Triticeae. *PNAS* 106, 15780–15785. doi: 10.1073/pnas.0908195106
- Lysak, M. A., Berr, A., Pecinka, A., Schmidt, R., McBreen, K., and Schubert, I. (2006). Mechanisms of chromosome number reduction in *Arabidopsis thaliana* and related Brassicaceae species. *PNAS* 103, 5224–5229. doi: 10.1073/pnas.0510791103
- Ma, X. F., and Gustafson, J. (2005). Genome evolution of allopolyploids: a process of cytological and genetic diploidization. *Cytogenet. Genome Res.* 109, 236–249. doi: 10.1159/000082406
- Macas, J., Novak, P., Pellicer, J., Cizkova, J., Koblizkova, A., Neumann, P., et al. (2015). In depth characterization of repetitive DNA in 23 plant genomes reveals sources of genome size variation in the legume tribe Fabaeae. *PLoS ONE* 10:e0143424. doi: 10.1371/journal.pone.0143424
- Majerová, E., Mandáková, T., Vu, G. T. H., Fajkus, J., Lysak, M. A., and Fojtová, M. (2014). Chromatin features of plant telomeric sequences at terminal vs. internal positions. *Front. Plant Sci.* 5:593. doi: 10.3389/fpls.2014.00593
- Mandáková, T., Hloušková, P., Koch, M. A., and Lysak, M. A. (2020). Genome evolution in Arabideae was marked by frequent centromere repositioning 32, 650–665. doi: 10.1105/tpc.19.00557
- Mandakova, T., Joly, S., Krzywinski, M., Mummenhoff, K., and Lysak, M. A. (2010). Fast diploidization in close mesopolyploid relatives of Arabidopsis. *Plant Cell* 22, 2277–2290. doi: 10.1105/tpc.110.074526
- Mandáková, T., and Lysak, M. A. (2008). Chromosomal phylogeny and karyotype evolution in x=7 *Crucifer* species (Brassicaceae). *Plant Cell* 20, 2559–2570. doi: 10.1105/tpc.108.062166
- Mandáková, T., and Lysak, M. A. (2018). Post-polyploid diploidization and diversification through dysploid changes. *Curr. Opin. Plant Biol.* 42, 55–65. doi: 10.1016/j.pbi.2018.03.001
- Mandáková, T., Pouch, M., Brock, J. R., Al-Shehbaz, I. A., and Lysak, M. A. (2019). Origin and evolution of diploid and allopolyploid camelina genomes were accompanied by chromosome shattering. *Plant Cell* 31, 2596–2612. doi: 10.1105/tpc.19.00366
- Mandáková, T., Pouch, M., Harmanová, K., Zhan, S. H., Mayrose, I., and Lysak, M. A. (2017). Multispeed genome diploidization and diversification after an ancient allopolyploidization. *Mol. Ecol.* 26, 6445–6462. doi: 10.1111/mec.14379
- Marazzi, B., Endress, P. K., Queiroz, L. P., and Conti, E. (2006). Phylogenetic relationships within *Senna* (Leguminosae, Cassiinae) based on three chloroplast DNA regions: patterns in the evolution of floral symmetry and extrafloral nectaries. *Am. J. Bot.* 93, 288–303. doi: 10.3732/ajb.93.2.288
- Mehrotra, S., and Goyal, V. (2014). repetitive sequences in plant nuclear dna: types, distribution, evolution and function. *Genom. Proteom. Bioinform.* 12, 164–171. doi: 10.1016/j.gpb.2014.07.003
- Murat, F., Armero, A., Pont, C., Klopp, C., and Salse, J. (2017). Reconstructing the genome of the most recent common ancestor of flowering plants. *Nature Genet.* 49, 490–496. doi: 10.1038/ng.3813
- Murat, F., Xu, J.-H., Tannier, E., Abrouk, M., Guilhot, N., Pont, C., et al. (2010). Ancestral grass karyotype reconstruction unravels new mechanisms of genome shuffling as a source of plant Evolution 20, 1545–1557. doi: 10.1101/gr.109744.110
- Novák, P., Robledillo, L. A., Koblizkova, A., Vrbová, I., Neumann, P., and Macas, J. (2017). TAREAN: a computational tool for identification and characterization of satellite DNA from unassembled short reads. *Nucleic Acids Res.* 45:e111. doi: 10.1093/nar/gkx257
- Ohri, D., Kumar, A., and Pal, M. (1986). Correlations between 2C DNA values and habit in *Cassia* (Leguminosae:Caesalpinioideae). *Plant Syst. Evol.* 153, 223–227. doi: 10.1007/BF00983689
- Okada, T., Ohzeki, J.-i., Nakano, M., Yoda, K., Brinkley, W. R., Larionov, V., et al. (2007). CENP-B controls centromere formation depending on the chromatin context. *Cell* 131, 1287–1300. doi: 10.1016/j.cell.2007.10.045
- Pellerin, R., Waminal, N., and Kim, H. (2019). FISH mapping of rDNA and telomeric repeats in 10 *Senna* species. *Hortic. Environ. Biotechnol.* 60, 253–260. doi: 10.1007/s13580-018-0115-y
- Pellestor, F., and Gatinois, V. (2018). Chromoanasythesis: another way for the formation of complex chromosomal abnormalities in human reproduction. *Hum. Reprod.* 33, 1381–1387. doi: 10.1093/humrep/dey231
- Pellestor, F., and Gatinois, V. (2020). Chromoanagenesis: a piece of the macroevolution scenario. *Mol. Cytogenet.* 13:3. doi: 10.1186/s13039-020-0470-0



- Perumal, S., Waminal, N. E., Lee, J., Lee, J., Choi, B. S., Kim, H. H., et al. (2017). Elucidating the major hidden genomic components of the A, C, and AC genomes and their influence on *Brassica* evolution. *Sci. Rep.* 7:17986. doi: 10.1038/s41598-017-18048-9
- Puri, B. K. (2018). The potential medicinal uses of *Cassia tora* linn leaf and seed extracts. *Rev. Recent Clin. Trials* 13, 3–4. doi: 10.2174/157488711301180131145359
- Resende, K., Prado, C., Davide, L., and Torres, G. J. T. J. o. B. (2014). Polyploidy and apomixis in accessions of *Senna rugosa* (G. Don). *HS Irwin Barneby* 38, 510–515. doi: 10.3906/biy-1312-66
- Rosato, M., Álvarez, I., Feliner, G. N., and Rosselló, J.A. (2018). Inter- and intraspecific hypervariability in interstitial telomeric-like repeats (TTTAGGG)n in *Anacyclus* (Asteraceae). *Ann. Bot.* 122, 387–395. doi: 10.1093/aob/mcy079
- Rousselet, J., Monti, L., Auger-Rozenberg, M. A., Parker, J. S., and Lemeunier, F. (2000). Chromosome fission associated with growth of ribosomal DNA in *Neodiprion abietis* (Hymenoptera: Diprionidae). *Proceed. Biol. Sci.* 267, 1819–1823. doi: 10.1098/rspb.2000.1216
- Ruban, A., Fuchs, J., Marques, A., Schubert, V., Soloviev, A., Raskina, O., et al. (2014). B chromosomes of *Aegilops speltoides* are enriched in organelle genome-derived sequences. *PLoS ONE* 9:e90214. doi: 10.1371/journal.pone.0090214
- Ruiz-Ruano, F. J., López-León, M. D., Cabrero, J., and Camacho, J. P. M. (2016). High-throughput analysis of the satellitome illuminates satellite DNA evolution. *Sci. Rep.* 6:28333. doi: 10.1038/srep28333
- Salsler, W., Bowen, S., Browne, D., el-Adli, F., Fedoroff, N., Fry, K., et al. (1976). Investigation of the organization of mammalian chromosomes at the DNA sequence level. *Fed. Proc.* 35, 23–35.
- Schubert, I. (2018). What is behind “centromere repositioning”? *Chromosoma* 127, 229–234. doi: 10.1007/s00412-018-0672-y
- Schubert, I., and Lysak, M. A. (2011). Interpretation of karyotype evolution should consider chromosome structural constraints. *Trends Genetics* 27, 207–216. doi: 10.1016/j.tig.2011.03.004
- Schubert, I., and Vu, G. T. H. (2016). Genome stability and evolution: attempting a holistic view. *Trends Plant Sci.* 21, 749–757. doi: 10.1016/j.tplants.2016.06.003
- Schubert, V., Neumann, P., Marques, A., Heckmann, S., Macas, J., Pedrosa-Harand, A., et al. (2020). Super-resolution microscopy reveals diversity of plant centromere architecture. *Int. J. Mol. Sci.* 21:3488. doi: 10.3390/ijms21103488
- Sharma, S., and Raina, S. N. (2005). Organization and evolution of highly repeated satellite DNA sequences in plant chromosomes. *Cytogenet. Genome Res.* 109, 15–26. doi: 10.1159/000082377
- Shatskikh, A. S., Kotov, A. A., Adashev, V. E., Bazylev, S. S., and Olenina, L. V. (2020). Functional significance of satellite DNAs: insights from *Drosophila*. 8:312. doi: 10.3389/fcell.2020.00312
- Soltis, P. S., and Soltis, D. E. (2016). Ancient WGD events as drivers of key innovations in angiosperms. *Curr. Opin. Plant Biol.* 30, 159–165. doi: 10.1016/j.pbi.2016.03.015
- Sousa, A., and Renner, S. S. (2015). Interstitial telomere-like repeats in the monocot family Araceae. *Bot. J. Linn. Soc.* 177, 15–26. doi: 10.1111/boj.12231
- Symonds, V. V., Soltis, P. S., and Soltis, D. E. (2010). Dynamics of polyploid formation in *Tragopogon* (Asteraceae): recurrent formation, gene flow, and population structure. *Evolution* 64, 1984–2003. doi: 10.1111/j.1558-5646.2010.00978.x
- Szymanski, M., Zielezinski, A., Barciszewski, J., Erdmann, V. A., and Karlowski, W. M. (2016). 5SRNADB: an information resource for 5S ribosomal RNAs. *Nucleic Acids Res.* 44, D180–D183. doi: 10.1093/nar/gkv1081
- Vrana, J., Simkova, H., Kubalaková, M., Cihalikova, J., and Dolezel, J. (2012). Flow cytometric chromosome sorting in plants: the next generation. *Methods* 57, 331–337. doi: 10.1016/j.ymeth.2012.03.006
- Waminal, N., Park, H. M., Ryu, K. B., Kim, J. H., Yang, T. J., and Kim, H. H. (2012). Karyotype analysis of *Panax ginseng* C.A.Meyer, 1843 (Araliaceae) based on rDNA loci and DAPI band distribution. *Comp. Cytogenet.* 6, 425–441. doi: 10.3897/CompCytogen.v6i4.3740
- Waminal, N. E., Pellerin, R. J., Kim, N.-S., Jayakodi, M., Park, J. Y., Yang, T.-J., et al. (2018a). Rapid and efficient FISH using pre-labeled oligomer probes. *Sci. Rep.* 8:8224. doi: 10.1038/s41598-018-26667-z
- Waminal, N. E., Perumal, S., Lee, J., Kim, H. H., and Yang, T.-J. (2016). Repeat evolution in *Brassica rapa* (AA), *B. oleracea* (CC), and *B. napus* (AACC) genomes. *Plant Breed. Biotech.* 4, 107–122. doi: 10.9787/PBB.2016.4.2.107
- Waminal, N. E., Perumal, S., Liu, S., Chalhoub, B., Kim, H. H., and Yang, T.-J. (2018b). “Quantity, distribution, and evolution of major repeats in *Brassica napus*,” in *The Brassica napus Genome*, eds S. Liu, R. Snowdon, and B. Chalhoub (Cham: Springer International Publishing), 111–129. doi: 10.1007/978-3-319-43694-4\_6
- Waminal, N. E., Yang, T.-J., In, J.-G., and Kim, H. H. (2020). Five-color fluorescence in situ hybridization system for karyotyping of *Panax ginseng*. *Horticult. Environ. Biotechnol.* 61, 869–877. doi: 10.1007/s13580-020-00267-1
- Wicker, T., Sabot, F., Hua-Van, A., Bennetzen, J. L., Capy, P., Chalhoub, B., et al. (2007). A unified classification system for eukaryotic transposable elements. *Nat. Rev. Genet.* 8, 973–982. doi: 10.1038/nrg2165
- Zellinger, B., Akimcheva, S., Puizina, J., Schirato, M., and Riha, K. (2007). Ku suppresses formation of telomeric circles and alternative telomere lengthening in *Arabidopsis*. *Mol. Cell* 27, 163–169. doi: 10.1016/j.molcel.2007.05.025

**Conflict of Interest:** The authors declare that the research was conducted in the absence of any commercial or financial relationships that could be construed as a potential conflict of interest.

Copyright © 2021 Waminal, Pellerin, Kang and Kim. This is an open-access article distributed under the terms of the Creative Commons Attribution License (CC BY). The use, distribution or reproduction in other forums is permitted, provided the original author(s) and the copyright owner(s) are credited and that the original publication in this journal is cited, in accordance with accepted academic practice. No use, distribution or reproduction is permitted which does not comply with these terms.